Bulletin of Electrical Engineering and Informatics
Vol. 14, No. 4, August 2025, pp. 2471~2487
ISSN: 2302-9285, DOI: 10.11591/eei.v14i4.9350

Optimal power control for wind/solar hybrid energy system based on multi-objective particle swarm optimization

Ratna Ika Putri[1], Ferdian Ronilaya[1], Ika Noer Syamsiana[1], Zakiyah Amalia[2], Lie Jasa[3]
[1]Department of Electrical Engineering, State Polytechnic of Malang, Malang, Indonesia
[2]Department of Mechanical Engineering, State Polytechnic of Malang, Malang, Indonesia
[3]Department of Electrical Engineering, Faculty of Engineering, Udayana University, Bali, Indonesia

Article Info

Article history:

Received Sep 24, 2024
Revised Apr 8, 2025
Accepted May 27, 2025

Keywords:

Hybrid energy
Multi-objective particle swarm optimization
Optimal power control
Photovoltaic
Wind turbine

ABSTRACT

The effectiveness of wind and solar energy as electricity generators is significantly impacted by unpredictable and varied environmental circumstances, which affect the output power of the wind-solar hybrid power generation system. So, a control system is required for the optimal power production of hybrid renewable energy systems (HRES). This study delineates optimal power management in wind/solar hybrid energy systems by the application of multi-objective particle swarm optimization (MOPSO) algorithms, inverter controllers, and battery controllers. The MOPSO algorithm enhances power generation by modifying the duty cycle of the direct current (DC)/DC converter based on the output from the wind turbine and photovoltaic (PV) system. The proportional-integral (PI) controller functions as both an inverter and battery controller to ensure the constancy of the DC link voltage and output power. The efficacy of the developed control was evaluated using simulation. A comparison has been conducted between the efficacy of the MOPSO algorithm and the perturb and observe (P&O) approach. The simulation findings indicate that the MOPSO algorithm surpasses the P&O method for performance and output power. The output power produced by HRES with the MOPSO algorithm exceeds that of the P&O approach. Optimal power control utilizing MOPSO can yield optimal power despite fluctuations in wind and solar intensity.

Corresponding Author:

Ratna Ika Putri
Department of Electrical Engineering, State Polytechnic of Malang, Indonesia
St. Soekarno Hatta 9, Malang, Indonesia
Email: ratna.ika@polinema.ac.id

1. INTRODUCTION

As fossil resources become scarce while remaining the main source of electricity generation, energy diversification is required. An initiative to diversify Indonesia's energy sources includes utilising renewable energy sources (RES) that are abundantly available. The use of renewable energy can reduce air pollution, is environmentally friendly and is available indefinitely. However, renewable energy is strongly influenced by environmental conditions and cannot be predicted so it takes the integration of several RES to provide the load with a constant supply of electrical energy. Hybrid wind and solar energy systems have been widely developed and researched to improve system performance and efficiency [1]-[3]. The output power in this system is strongly influenced by erratic wind speed and solar irradiation so it will produce fluctuating output power. To enhance the efficiency of this system, one can utilize an optimization method to adapt the converter. This will enable it to extract the greatest amount of power, even in the presence of fluctuations in wind and irradiation [4]-[6].

There are multiple strategies available to optimize the efficiency of electricity generation in wind-solar hybrid systems. In this system, the constant voltage method was employed to ensure a consistent voltage while attempting to charge the batteries by adjusting the direct current (DC)/DC converter duty cycle. The constant voltage approach produces significant oscillations and requires a significant amount of time to achieve a steady state [7]. To overcome the limitations of the constant voltage approach, the perturb and observe (P&O) method was devised and implemented in a hybrid system that utilizes batteries for energy storage. This approach offers enhanced dynamic response to fluctuations in wind and solar radiation. However, its efficacy is highly contingent upon the chosen step size. The P&O approach, when used with wind turbines and PV systems, is capable of rapidly tracking maximum power. However, it also generates oscillations [8], [9]. Additionally, particle swarm optimization (PSO) is used to enhance the output power of photovoltaic (PV) systems and to determine the optimal design parameter for adjusting the step size in the P&O and incremental conductance (IC) methods [10]. The IC method is also applied PV systems, although it is more complex [11]. The P&O method is modified to reduce oscillations by adjusting the step size and modified method produces better performance. Adaptive P&O has been tested on wind turbine systems (WTS), PV systems, and wind-solar hybrid systems [12]-[14]. According to the test results, this algorithm can reduce oscillations and extract more maximum power regardless of wind speed or solar irradiation.

Furthermore, the maximum power extraction technique in RES has been developed by integrating artificial intelligence and swarm algorithms. Through the utilisation of neural networks and fuzzy algorithms in wind and PV turbines, maximum power can be extracted and improved performance can be achieved [15], [16]. PSO and firefly swarm algorithms have also been used in hybrid systems, resulting in operational cost optimization [17]-[20]. The analysis conducted on various maximum power point tracking (MPPT) techniques for different renewable energy systems indicates that the artificial intelligence-based hybrid MPPT technique demonstrates better results compared to other methods [6]. Batteries are commonly employed for energy storage in RES to minimize variations in generated output power. Utilizing batteries may effectively mitigate fluctuations in wind speed and irradiation, hence ensuring a stable output power. The battery can be used to store excess power generated by the energy source. Later, when the power generated is insufficient, the battery can supply the load [12], [21]-[25].

This article presents the development of a multi-objective particle swarm optimization (MOPSO) algorithm to optimize input power in an off-grid hybrid wind-solar system with an alternating current (AC) load. The system features a battery for energy storage and a voltage source inverter (VSI) to deliver AC power. MOPSO aims to maximize power output from wind and PV sources by adjusting the DC/DC converter duty cycle. Its performance is compared with the conventional P&O method.

2. METHOD

This study methodology is executed in multiple phases, including hybrid renewable energy systems (HRES) system design, HRES modeling, optimal power control design for HRES, and control algorithm evaluation by simulation. Optimal power management in HRES comprises three components: inverter regulation via a proportional-integral (PI) controller, battery management via a PI controller, and the MOPSO algorithm to maximize power output in HRES. The system's ideal power generation is significantly affected by wind speed and irradiation conditions. Optimal power control performance testing is conducted through simulations under two conditions: constant wind speed and irradiance, and variable wind speed and irradiance.

2.1. Modelling of solar/wind hybrid energy system

A hybrid wind-solar RES consists of a wind turbine, PV system, inverter, inverter controller, bidirectional converter, battery controller, maximum power extraction system, and battery, as shown in Figure 1. The wind turbine uses a rectifier and DC/DC converter, while the PV system connects directly to a DC/DC converter. The MOPSO algorithm optimizes output by adjusting the converter’s duty cycle. A VSI supplies 4000 W AC power, controlled to match load requirements.

A bidirectional converter is a two-way converter that connects the battery to the system via the settings on the battery controller. Charging and discharging of the battery is controlled by the battery controller in order to maintain a consistent energy level at a specified value. The DC link voltage is set constant at 400 V. The battery output power is contingent upon the WTS and PV power sources.

2.2. Modelling of wind turbine energy system

The WTS comprises a wind turbine and a generator. The gathered wind energy will be harnessed to operate a generator, generating electrical energy in direct proportion to the amount of wind energy captured. This article employs a permanent magnet synchronous generator (PMSG). The application of WTS modeling

in the design and development of controls enables the achievement of optimal and precise performance. The wind turbine model elucidates the correlation between the input of a wind turbine and the power torque generated by the wind turbine. The torque of a wind turbine is subject to a number of influencing factors, including turbine speed, rotor blades, pitch angle, turbine size and form, turbine area, and wind speed. In (1) illustrates the calculation of the power generated by the wind turbine.

$$P_m = \frac{1}{2}\rho\pi R^5 \frac{\omega r^3}{\lambda^3} C_p \quad (1)$$

Cp represents the coefficient of power conversion in the turbine, λ denotes the tip speed ratio, β refers to the pitch angle, R represents the radius of the turbine, and v represents the wind speed. The tip speed ratio (λ) is defined as the ratio of the angular speed of the turbine to the speed of the wind. This relationship is mathematically represented by (2):

$$\lambda = \frac{\omega_r R}{v} \quad (2)$$

ω_r represents the angular velocity of the turbine. Figure 2 illustrates the relationship between the mechanical output power of a wind turbine and the turbine speed, taking into account diverse wind speeds and a pitch angle of 0 degrees.

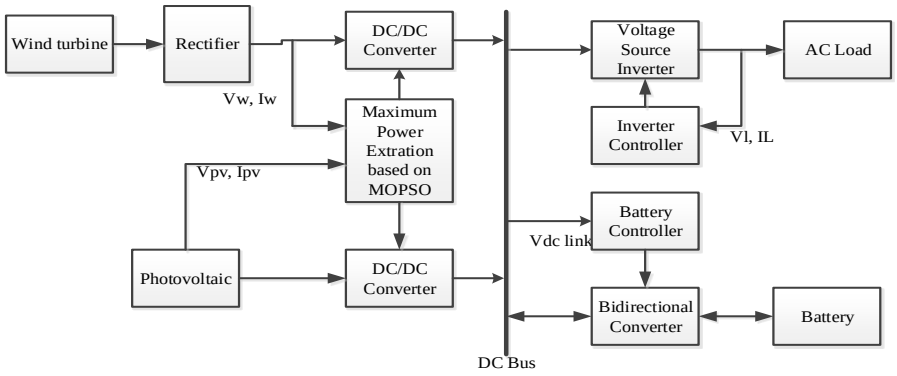

Figure 1. Solar/wind HRES

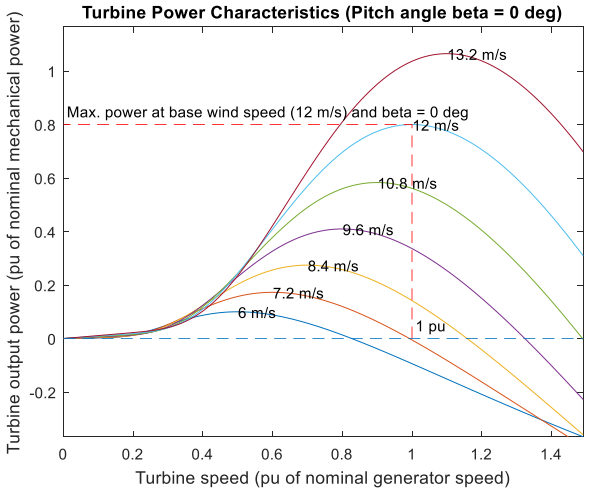

Figure 2. Wind turbine characteristics

The wind turbine's greatest power output is contingent upon the wind speed. The mechanical torque of the turbine can be computed using (3):

$$T_m = 0.5\rho A \frac{C_p(\lambda,\beta)}{\lambda} v^2 \quad (3)$$

The mathematical representation of the behavior of a wind turbine can be described by an equation that considers its dynamic properties.

$$\frac{d\omega_r}{dt} = \frac{1}{J}[T_m - T_L - F\omega_r] \quad (4)$$

J denotes the moment of inertia, F represents the friction coefficient, Tm represents the turbine torque, and T_L indicates the torque alternator associated with the turbine. The conversion of motion energy into electrical energy can be achieved by utilizing the dynamic PMSG model, which can be represented by the analogous dq circuit depicted in Figure 3. The dq-axis model of the PMSG electrical circuit consists of the d-axis component depicted in Figure 3(a) and the q-axis component depicted in Figure 3(b).

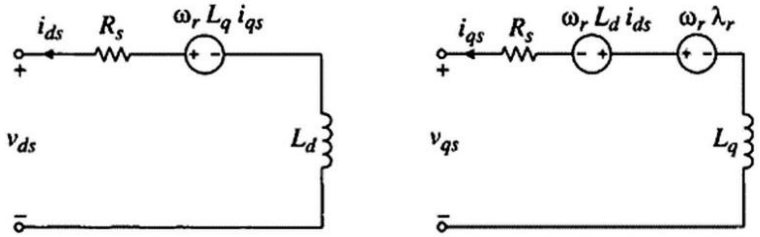

(a) (b)

Figure 3. PMSG simple model in dq-axis; (a) d-axis circuit and (b) q-axis circuit

The electromagnetic torque produced by a PMSG can be calculated using (5):

$$T_e = \frac{3P}{2}\left(i_{qs}\lambda_r + i_{ds}i_{qs}(L_d + L_q)\right) \quad (5)$$

2.3. Modeling of solar energy system

The PV has many interconnected solar cells that transform solar energy into DC. The PV properties exhibit a significant degree of non-linearity and are influenced by external variables such as sun irradiance and temperature. Figure 4 illustrates the PV characteristics suggested in this research report. The PV system has a capacity of 3.5 kilowatts and is equipped with DC/DC converter. The MOPSO algorithm is employed to optimize the duty ratio of DC/DC converter in the MPPT controller, hence enhancing the system efficiency. The MPPT algorithm determines the duty cycle by analyzing the measurements of current and voltage from the PV system.

Simulation testing is necessary to assess the performance of the MPPT algorithm, thereby requiring the usage of PV modeling. PV systems are composed of numerous interconnected cells, arranged in both series and parallel configurations, to provide the requisite power output. The system can be represented by the single diode model. The relationship between the current and voltage of the PV system in the mentioned model is given as (6):

$$I = I_{PH} - I_{sat}\left[e^{q\frac{V_{PV}+I_{PV}.R_S}{F.K.T}} - 1\right] - \frac{V_{PV}+I_{PV}.R_S}{R_{SH}} \quad (6)$$

V_{PV} represents the voltage (V) of the PV output. I_{PV} represents the current (A) of the PV output. I_{PH} represents the current (A) generated by light. F represents the ideality factor. K represents Boltzman's constant. T represents the ambient temperature (K). I_{sat} represents the reverse saturation current (A). q represents the charge of an electron. R_s represents the series resistance, and R_{sh} represents the shunt resistance.

2.4. Optimal power point tracking based on multi-objective particle swarm optimization

Based on the HRES presented in Figure 1, HRES has 3 control units, namely MOPSO-based MPPT, inverter control, and bidirectional control.

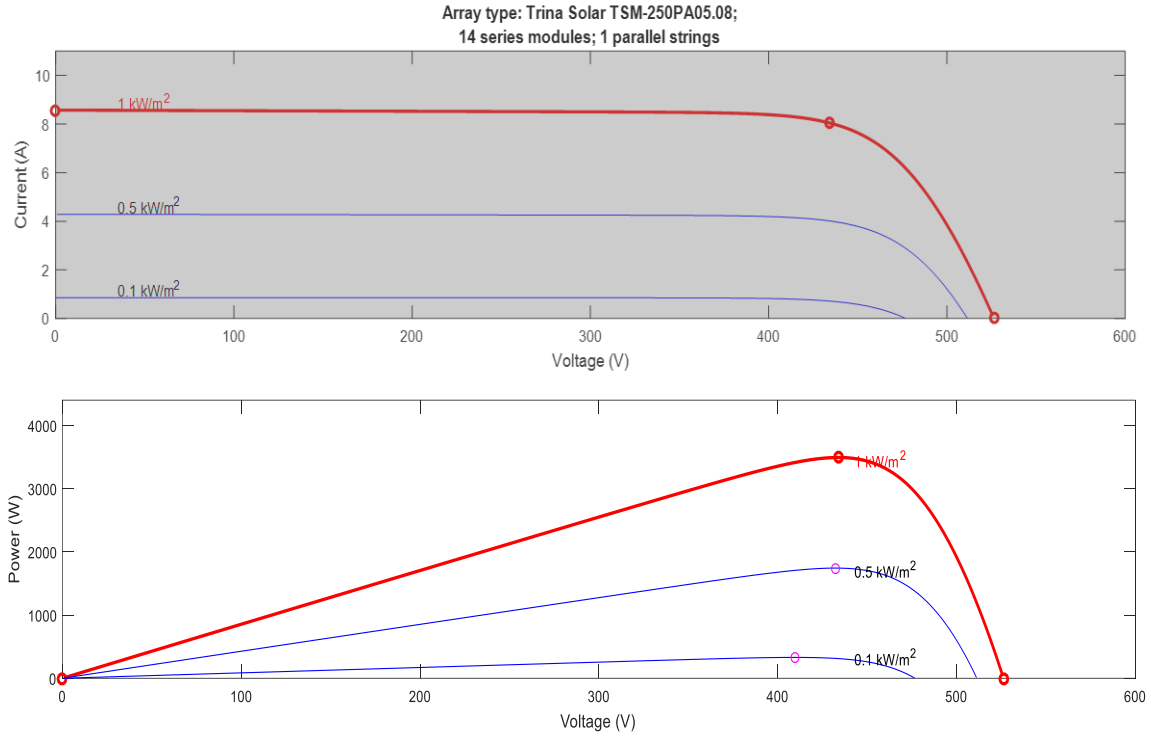

Figure 4. PV characteristic

2.4.1. Maximum power point tracking with multi-objective particle swarm optimization

This research utilizes the MOPSO algorithm to maximize the output power of the HRES wind-solar system. Wind-solar HRES stores excess power in batteries that are controlled by a battery controller and supplies power when the load requires it. VSI connects the system to the AC load. The MOPSO optimization algorithm draws inspiration from the behavior of ants, bees and birds. As an alternative to genetic algorithms, which are often referred to as evolution-based procedures, this swarm intelligence-based algorithm is referred to as a behaviorally inspired algorithm. MOPSO is employed to optimize the PI controller parameters of the bidirectional converter to ensure the constancy of the DC link voltage. The MOPSO algorithm demonstrates effective performance within the system [17], [18]. In this paper, MOPSO has two objective functions: optimal power in WTS and PV systems based on voltage and current converters in WTS and PV systems.

Each entity in this article is depicted as a particle with both a position and a velocity. Each particle navigates within a defined space by retaining the memory of its best previous position or comparing it to the value of the goal function. This information is then shared with other particles to update their own positions. The remaining particles within the group will adapt their location and velocity in accordance with this position. Each particle will interact with other particles to share and update information, resulting in personal best and global best values. Several parameters that affect the performance of this algorithm include the global learning rate (C_1 and C_2), which is given by C_1 and C_2 with values ranging from 0 to 1. Uniform random functions (R_1 and R_2) in the range 0 to 1.

The group's displacement is dictated by the learning rate and velocity. This MOPSO updates the duty cycle for each converter in the WTS and PV system based on an:

$$\Delta D_i^{k+1} = w\Delta D_i^k + C_1 r_1 \left(D_{Pbesti}^k - D_i^k\right) + C_2 r_2 \left(D_{Gbesti}^k - D_i^k\right) \quad (7)$$

$$D_i^{k+1} = D_i^k + \Delta D_i^k \quad (8)$$

w represent the momentum factor, r_1 and r_2 denote random values, C_1 and C_2 represent acceleration constants, D_i^k represents the current duty cycle, D_i^{k+1} represents a modified duty cycle, D_{Pbesti}^k represents the best duty cycle for each experiment, D_{Gbesti}^k represents the best duty cycle in the group, ΔD_i^k represents the current experiment speed, and ΔD_i^{k+1} represent the modified experiment speed. Figure 5 depicts the MOPSO flowchart. The MOPSO algorithm in the wind solar hybrid system yields two outputs: the duty cycle for the

converter in the PV system and the duty cycle for the WTS. The steps of the MOPSO algorithm are as follows:

- Initialization of MOPSO parameters includes setting the swarm size to 10 and the maximum step amount to 100. The values of other parameters are as follows: $w = 0.15$, $C_1 = 0.5$, $C_2 = 0.7$, and $\alpha = 0.01$.
- Calculate the output power of a PV system (P_{PV}) and a 3-phase rectifier (P_{WT}) by measuring the output voltage and current of the PV system and rectifier. Use the following:

$$P_{PV} = V_{PV} * I_{PV}$$

$$P_{WT} = V_{WT} * I_{WT}$$

  V_{PV} represents the output voltage of the PV system, V_{WT} represents the output voltage of the 3-phase rectifier, I_{PV} represents the output current of the PV system, and I_{WT} represents the output current of the 3-phase rectifier.
- Analyze the differences in power output between current and prior PV and wind turbine (WT) systems, focusing on the smallest power variations.
- Compare the duty cycle of the maximum step size with α.
- Determine the highest power value of the converter; the present power output of the converter is greater than that of the previous iteration, set the best individual value as the current power and the best individual duty cycle as the current duty cycle ($D_{pbest} = D_i$).
- The optimal herd value is determined by selecting the highest value from each experiment.
- Updating the duty cycle and step size duty cycle for each study based on (7) and (8).

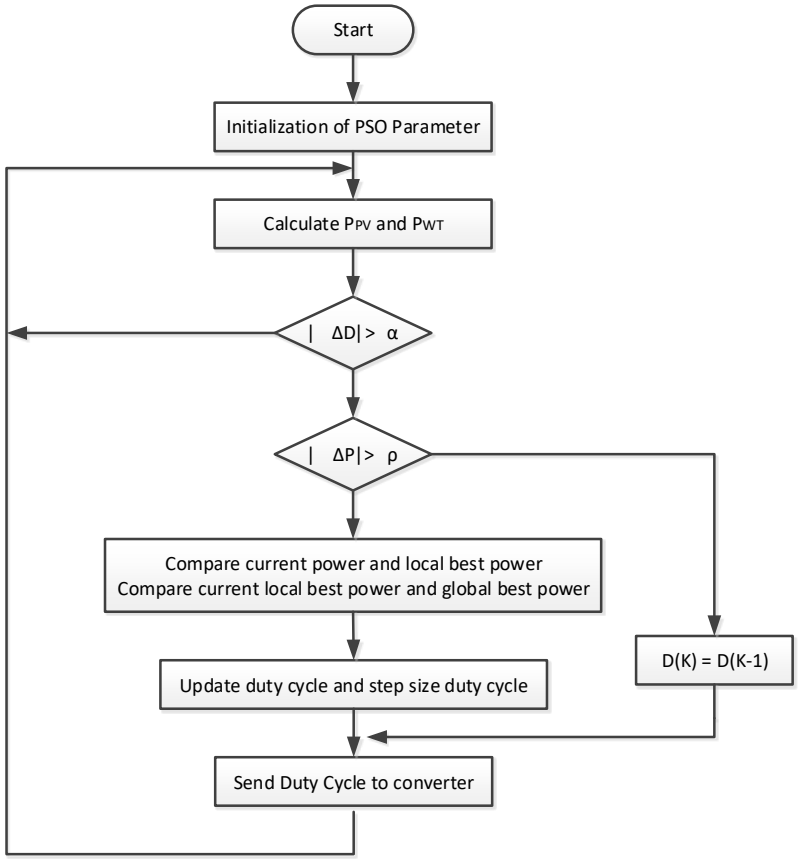

Figure 5. PSO algorithm flowchart

2.4.2. Inverter control

The inverter controller modifies the load power according to the requirements by utilizing the inverter's pulse width modulation (PWM) settings. The inverter circuit establishes a connection between the DC link and the load, transforming the DC power into AC voltage. The RL filter is linked to the inverter output in order to decrease noise and weaken the AC signal at the load. Figure 6 illustrates the components of the inverter controller, which include a PI controller that regulates the d-axis current, a PI controller that regulates the q-axis current, a phase-locked loop (PLL), and a PWM generator.

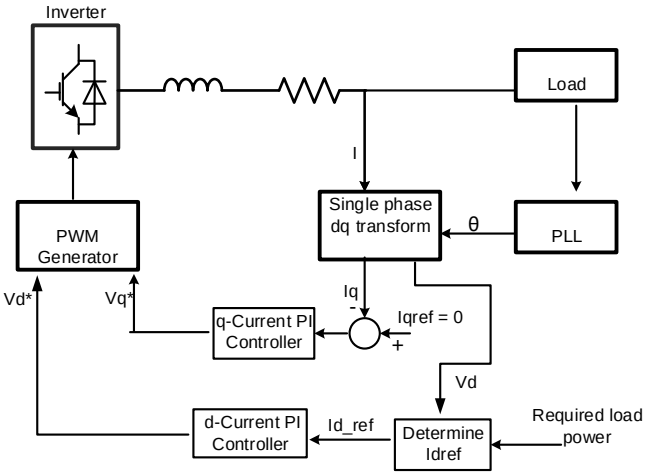

Figure 6. Inverter controller

The regulation of the d-axis and q-axis currents is accomplished through the utilization of a PI controller. The d-axis reference current ($i_{d_{ref}}$) is determined by (9), which takes into account the desired load power (P_{ref}).

$$i_{d_{ref}} = \frac{P_{ref}}{v_{dg}} \tag{9}$$

To achieve a power factor of unity, the q-axis reference current ($i_{q_{ref}}$) is adjusted to zero. In (10) and (11) represents the output of the control system for regulating the d-axis current (U_{pid}) and the q-axis current (U_{piq}).

$$v_d = U_{pid} - 2\omega_s L i_q + v_{dg} \tag{10}$$

$$v_q = U_{piq} + 2\omega_s L i_d + v_{qg} \tag{11}$$

By inserting (13) and (14) into the differential equations, the currents i_d and i_q can be represented as (12) and (13):

$$\frac{di_d}{dt} = -\frac{R}{L} i_d + \frac{1}{L} U_{pid} \tag{12}$$

$$\frac{di_q}{dt} = -\frac{R}{L} i_q + \frac{1}{L} U_{piq} \tag{13}$$

The transfer function equation for the change in the PI control output of the d-axis and q-axis current, stated in Laplace function form, can be written as (14):

$$H(s) = \frac{I_d(s)}{U_{pid}(s)} = \frac{I_q(s)}{U_{piq}(s)} = \frac{\frac{1}{R}}{\left(\frac{L}{R}\right)s+1} \tag{14}$$

The PI control system in the Laplace transform is expressed by:

$$U_{pi}(s) = K_p\left(1 + \frac{1}{T_{is}}\right)[I^*(s) - I(s)] \quad (15)$$

K_p represents the proportional gain, Ti represents the integrator gain, and I^* represents the reference current in the Laplace transformation. The closed-loop transfer function of the current control system for the d-axis and q-axis can be represented as (16):

$$H(s) = \frac{I(s)}{I^*(s)} = \frac{\left(\frac{1}{R}\right)Kp(s+\frac{1}{Ti})}{s\left(\left(\frac{L}{R}\right)s+1\right)+\left(\frac{1}{R}\right)Kp(s+\frac{1}{Ti})} \quad (16)$$

By using a filter resistance value (r) of 5 ω and an inductance of 2 mH, using the pole placement method, the values of $Kp = 0.5$ and $Ki = 10$ can be determined. As stated in (16), the parameter values for both controllers are the same.

2.4.3. Battery controller

The bidirectional buck-boost converter utilizes two insulated gate bipolar transistor (IGBT) switching components that alternate to connect the battery as an energy store to the DC-link voltage. A stand-alone solar wind HRES with an integral proportional controller is employed to modify the duty cycle of a bidirectional converter. The modelling results indicate that this converter is capable of maintaining stability in the DC link voltage during the battery's charging and discharging processes. As a result, the load receives a consistent output voltage even when there are fluctuations in wind speed and sun intensity. A bidirectional converter is designed for solar wind HRES, and based on simulation and experimental results, this converter can store energy in the battery while maintaining the load current and voltage. Several studies have also used bidirectional converters in solar wind HRES [21].

The primary objective of the bidirectional converter's regulation is to ensure the constant maintenance of the DC link voltage despite variations in wind speed and irradiation. This is accomplished through the regulation of the battery's charging and discharging cycles. The battery will undergo a process of recharge when the power output from the WTS and PV systems exceeds the power consumed by the load. Figure 7 illustrates how the controller of the bidirectional converter utilizes a PI controller, which is determined using the DC link voltage and the reference DC link voltage. In (17) can be used to determine the PI controller.

$$U(t) = K_p e(t) + K_i \int_0^t e(\tau)d\tau \quad (17)$$

The control signal, $U(t)$, is determined by the proportional gain, Kp, the integrator gain, Ki, the differentiator gain, Kd, and the error, $e(t)$. The output of the PID controller will be passed via a PWM generator in order to produce a duty cycle. The PID controller parameter values utilized in this study are $Kp = 25$, $Ki = 0.01$, and $Kd = 0$.

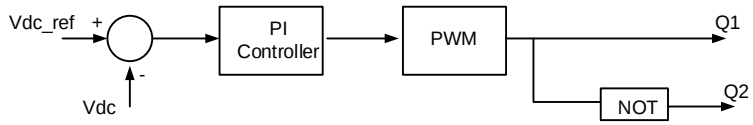

Figure 7. Bidirectional controller

3. RESULT AND DISCUSSION

Optimal power point tracking based on MOPSO on HRES with energy storage has been simulated. The MOPSO algorithm was evaluated under two scenarios: one in which wind speed and irradiation were maintained, and another in which they were subject to variation. The results of the MOPSO performance test were compared with the HRES system that use the P&O approach. The HRES system comprises two WTS and PV systems.

3.1. Case 1: wind speed and irradiance constant

The MOPSO algorithm was tested on an HRES with WTS and PV systems by providing 6 m/s wind speed and 500 w/m^2 irradiation. The test findings of the MOPSO algorithm were compared to those of the

P&O approach. Figure 8 compares the output power of the WTS using HRES with MOPSO and HRES with P&O. The WTS output power on HRES with MOPSO is 11250 W, while on P&O it is 10530 W. Furthermore, HRES with P&O produces more overshoot in transient conditions than MOPSO. Figure 9 illustrates the power generation of the PV system on HRES with MOPSO and P&O algorithms. The implementation of P&O in wind solar systems enhances power efficiency but induces oscillations in the generated electricity [21]. MOPSO surpasses P&O in terms of power generation. PV output power with P&O produces more oscillations than HRES with MOPSO.

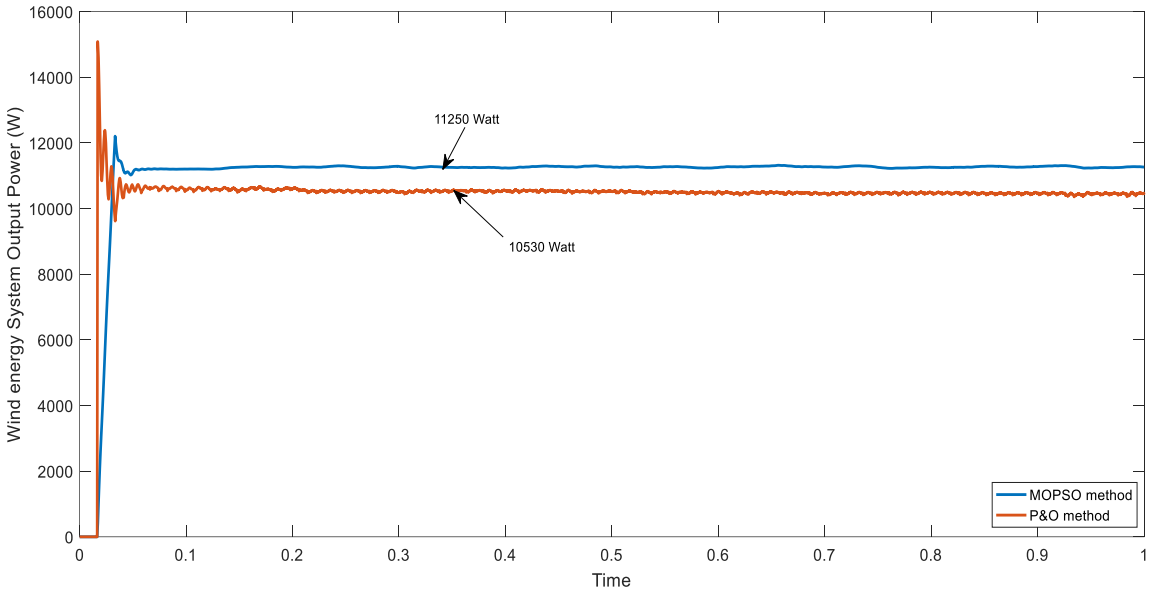

Figure 8. WTS output power using MOPSO and P&O method

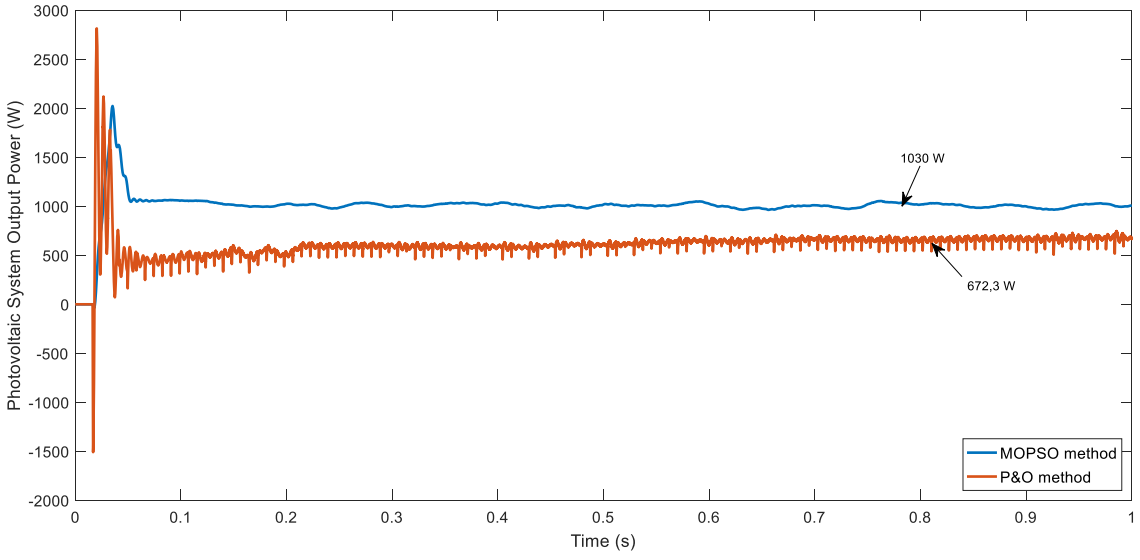

Figure 9. PV output power on HRES-based MOPSO and PO method

An effective method for regulating the DC link voltage at 400 V involves using a bidirectional converter with a PI controller in a HRES applying MOPSO and P&O techniques. Figure 10 shows the DC link response for both algorithms, demonstrating similar performance. This indicates the efficiency of the PI controller, consistent with previous studies that also achieved stable results using an adaptive PI controller [17]. By maintaining a constant DC voltage, it is possible to achieve an overshoot of 11.2% and a steady-

state inaccuracy of 0.5%. Figure 11 illustrates the power response of the load on HRES while utilizing MOPSO and P&O. The inverter controller ensures a consistent load power of 4000 W through the adjustment of the PWM duty cycle transmitted to the VSI circuit. The inverter controller is capable of maintaining a load power of 3981 W while maintaining a steady state error of 0.4%.

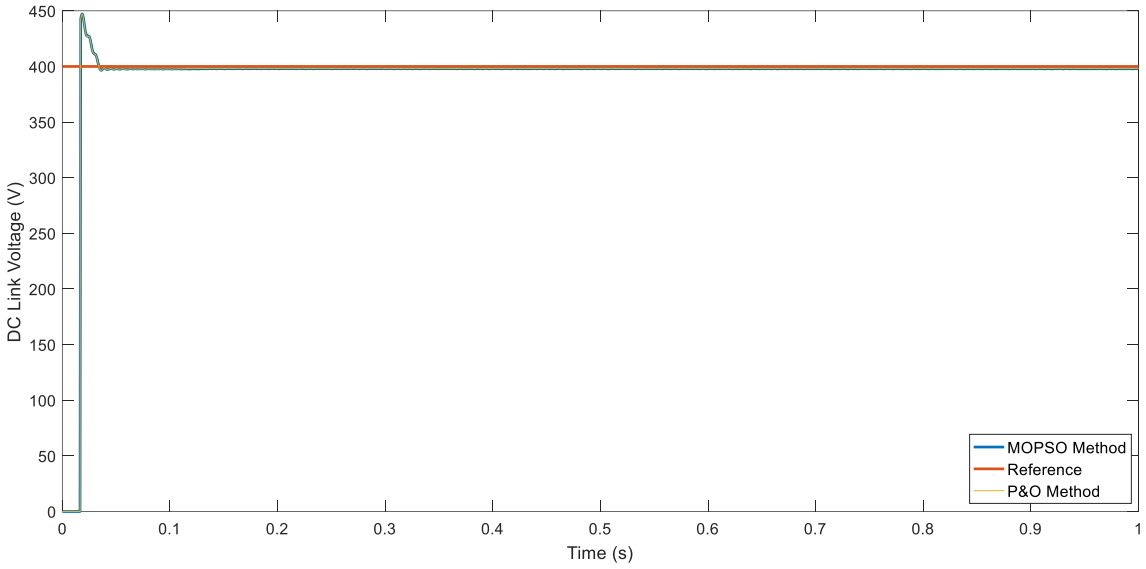

Figure 10. DC link voltage of HRES using MOPSO and PO method

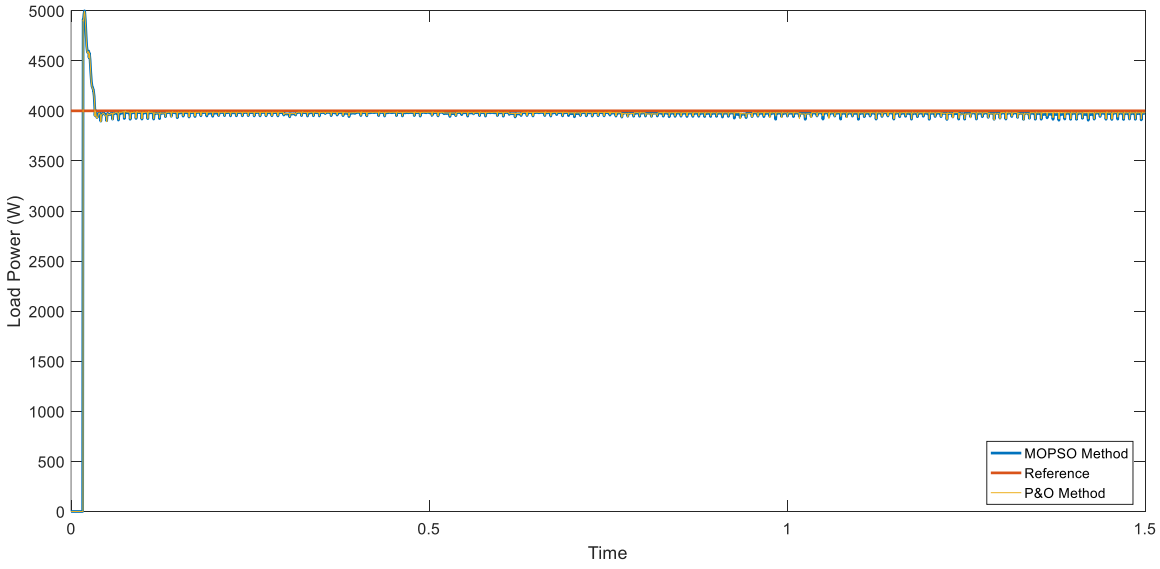

Figure 11. Load power of HRES using MOPSO and PO method

Figure 12 presents the power output of WTS, PV system, load, and battery. In the HRES utilizing MOPSO, the battery successfully stores 9800 W of excess energy. Conversely, the P&O-based HRES stores only 8091 W, as shown in Figure 13, due to the lower total power generated by the WTS and PV systems. This highlights the advantage of using MOPSO for maximizing energy capture. Researchers have explored various MPPT techniques, and hybrid approaches based on artificial intelligence, such as PSO, have demonstrated superior performance over traditional MPPT methods in renewable energy applications [6], [9].

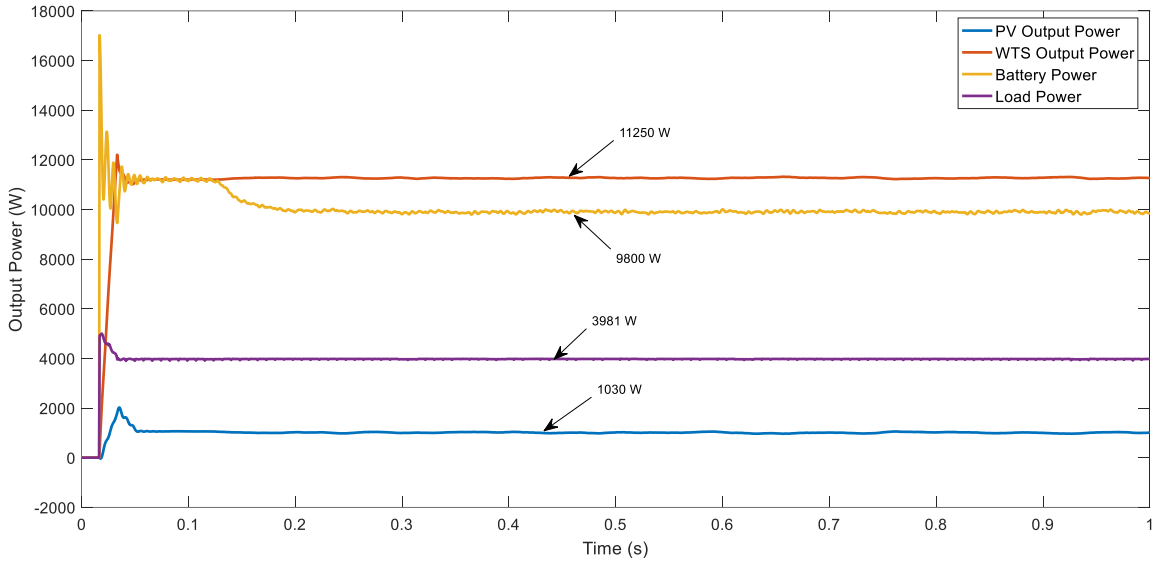

Figure 12. Output power of WTS, PV system, load, and battery on HRES Using MOPSO method

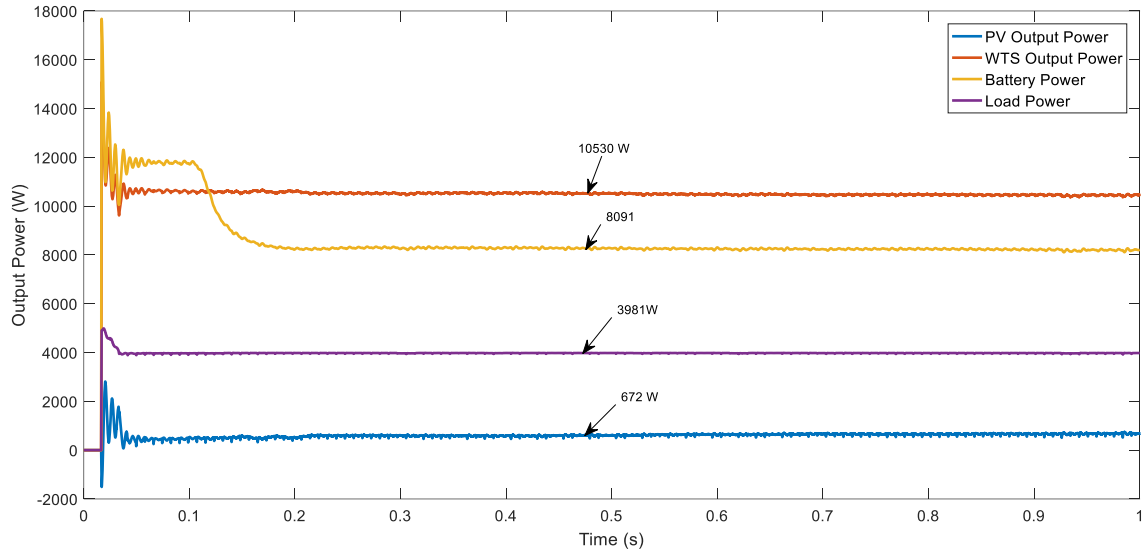

Figure 13. Output power of WTS, PV system, load, and battery on HRES using the PO method

3.2. Case 2: wind speed and irradiance changed

The optimal performance of power point tracking with MOPSO on HRES wind/solar is also simulated by giving changes in wind speed and irradiation. Figure 14(a) illustrates the change in wind speed, which decreases from 8 m/s to 5 m/s. Figure 14(b) illustrates a shift in solar irradiance from 500 W/m² to 750 W/m².

Figure 15 shows the WTS's output power using both the P&O and MOPSO methods. The changes in wind speed and irradiation are depicted in Figure 14. The MOPSO algorithm produces an output power that is higher than the power produced by the P&O technique. Figure 16 shows that the PV system output power is higher when the MOPSO method is utilized instead of the P&O method. The MOPSO technique is capable of optimizing power extraction under varying wind speed and irradiation conditions.

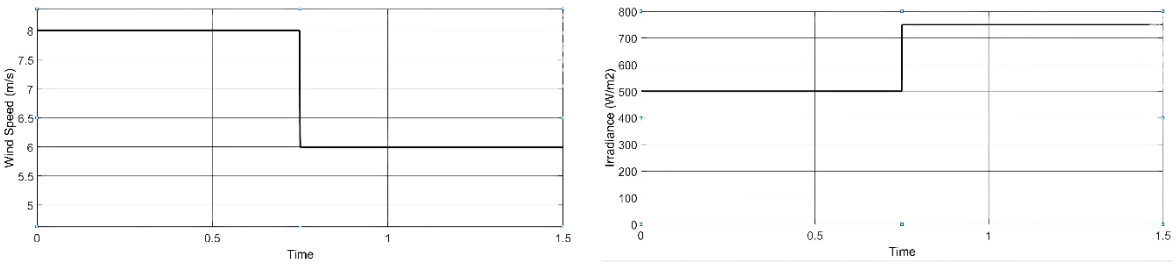

(a) (b)

Figure 14. Wind speed and irradiance profile: (a) wind speed changed and (b) irradiance changed

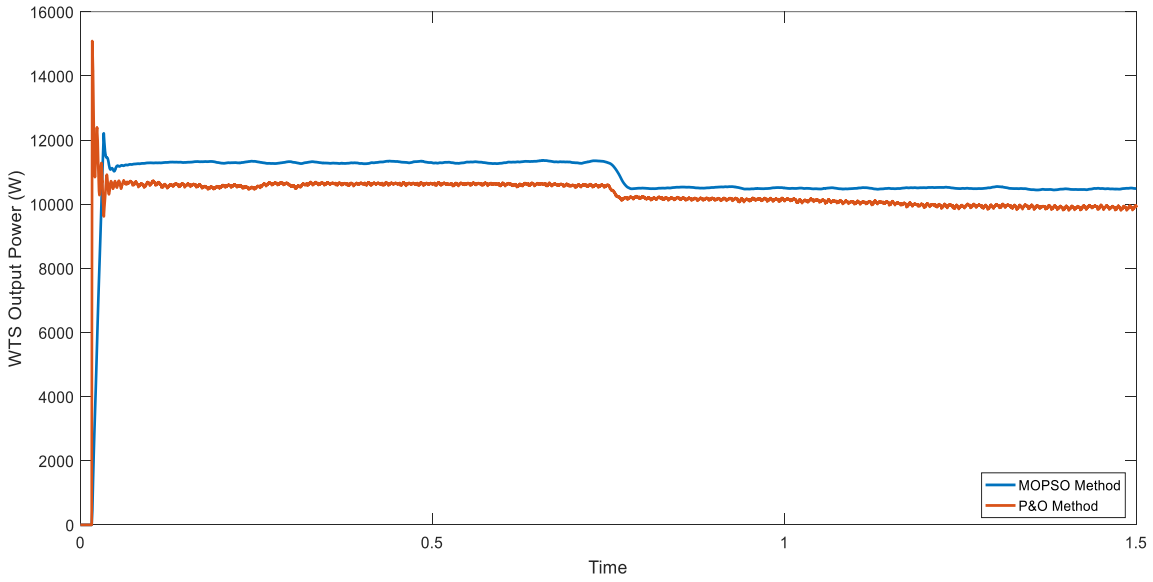

Figure 15. WTS output power of HRES using MOPSO and P&O method with wind speed and irradiance changed

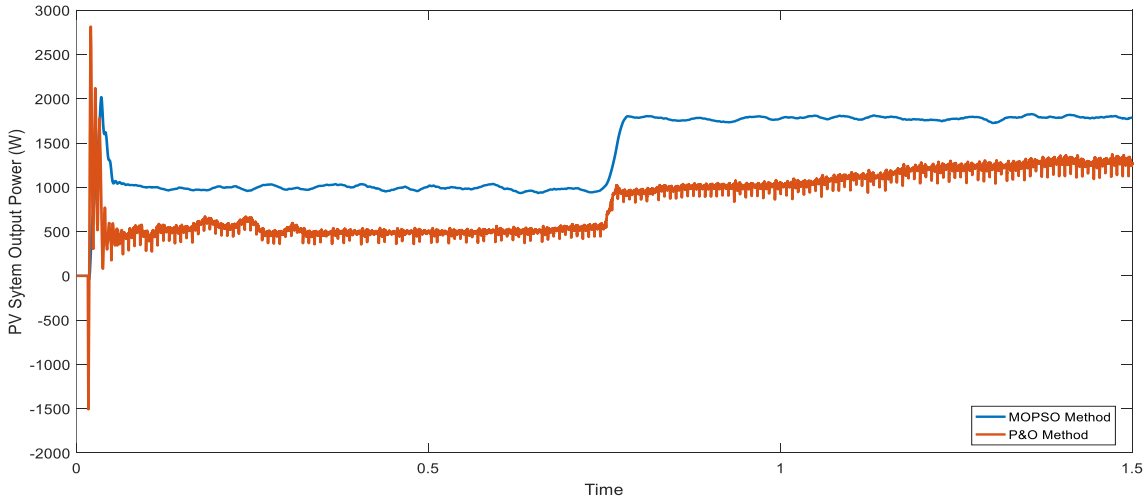

Figure 16. PV output power on HRES-based MOPSO and PO method with wind speed and irradiance changed

Figure 17 depicts the variation in DC link voltage resulting from fluctuations in wind speed and irradiance. The battery controller is capable of regulating a consistent DC link voltage, even in the presence of variations in irradiation, wind speed, and therefore, changes in the output power of the WTS and PV system. Similarly, the load power can be kept constant, as depicted in Figure 18. This demonstrates the effective performance of the inverter controller and battery controller in responding to fluctuations in wind speed and irradiation.

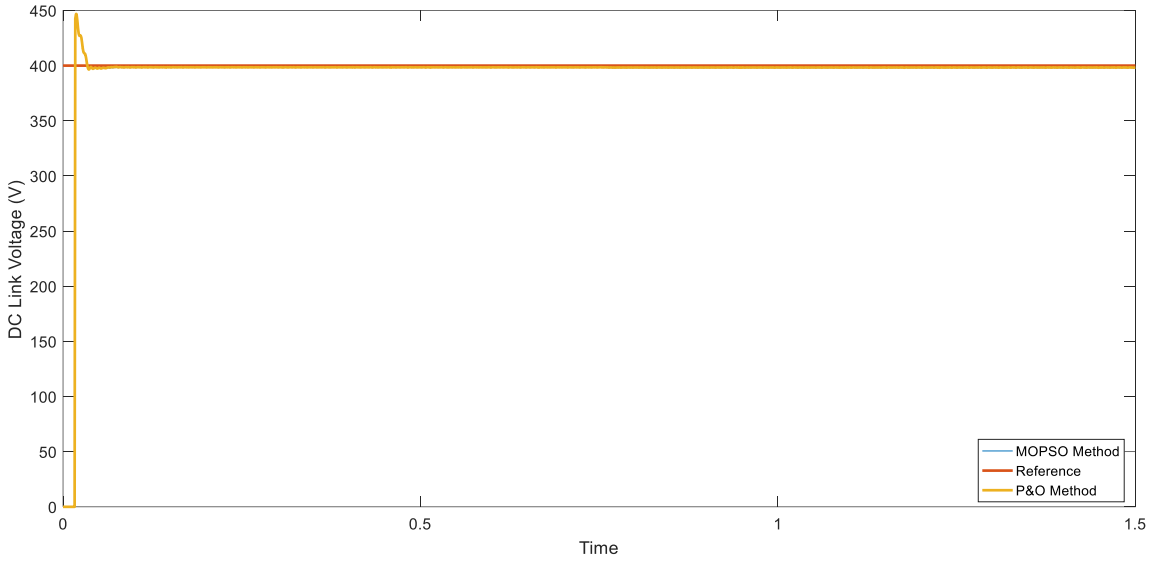

Figure 17. DC link voltage of HRES using MOPSO and PO method with wind speed and irradiance changed

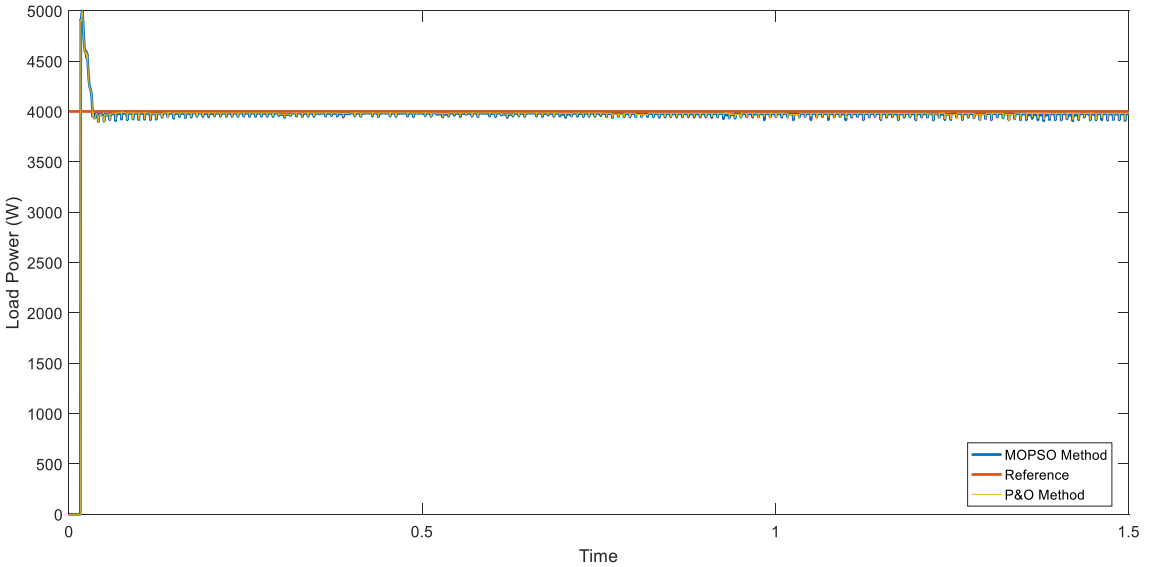

Figure 18. Load power of HRES using MOPSO and PO method with wind speed and irradiance changed

Figure 19 illustrates the power output produced by the WTS, PV system, load, and battery when subjected to variations in wind speed and irradiation, using the MOPSO approach. Figure 20 illustrates the power output obtained through the use of the P&O approach. The performance of MOPSO surpasses that of the P&O method due to its ability to extract a greater amount of power. So that the power stored in the battery in a system with MOPSO will be greater. The battery power level will fluctuate in response to variations in wind speed and irradiation, leading to corresponding changes in the output power of the WTS and PV systems.

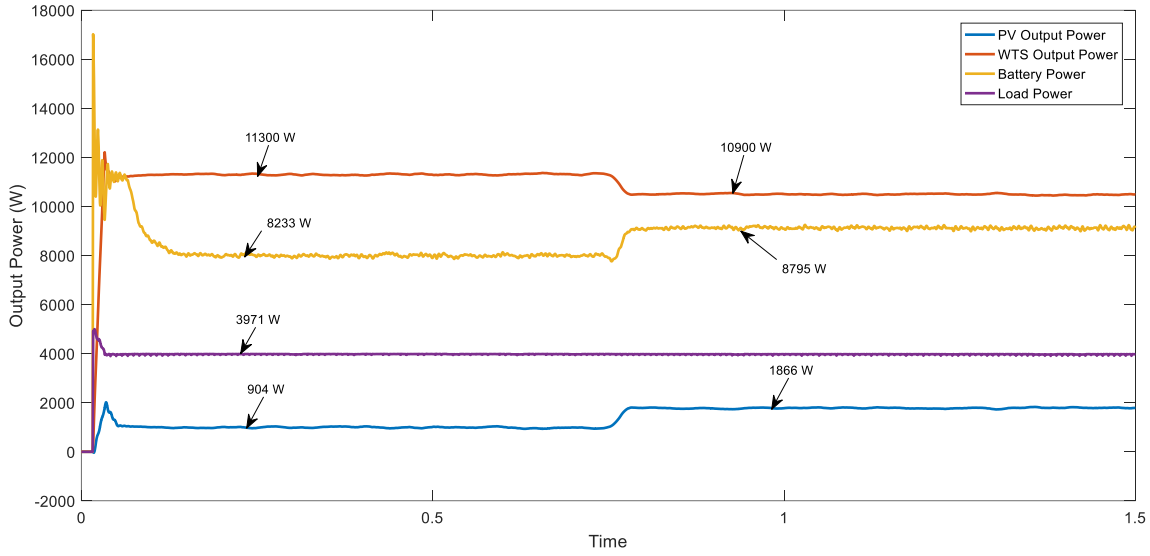

Figure 19. Output power of WTS, PV system, load, and battery on HRES using MOPSO method with wind speed and irradiance changed

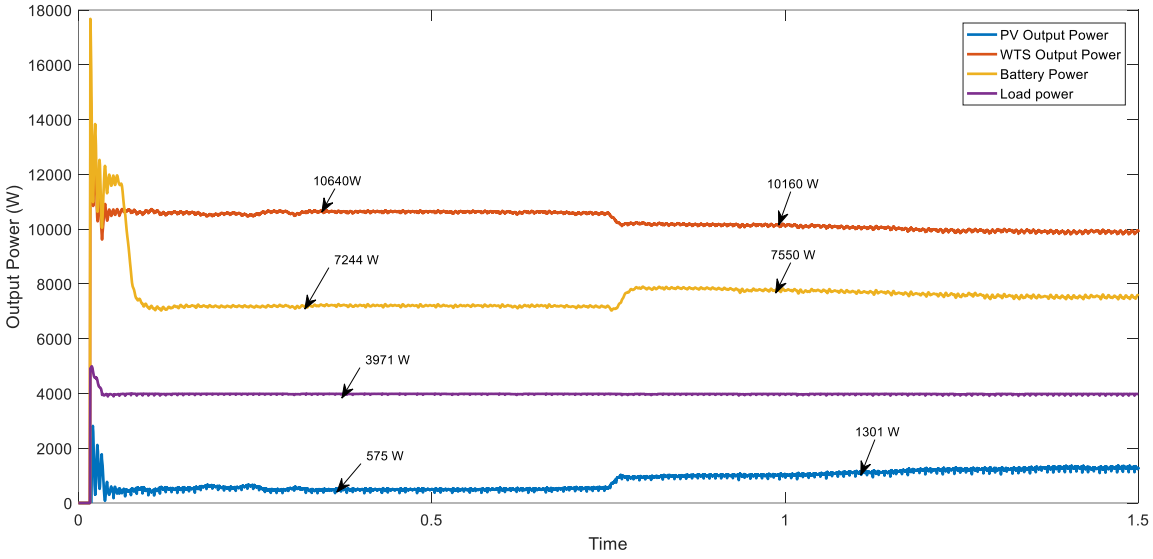

Figure 20. Output power of WTS, PV system, load, and battery on HRES using P&O method with wind speed and irradiance changed

4. CONCLUSION

This study presents the utilization of the MOPSO algorithm to achieve optimal controls for a solar-wind hybrid system and extract the highest power. A wind solar hybrid system is comprised of a WTS, PV system, inverter, inverter controller, bidirectional converter, battery controller, maximum power extraction, and battery. The MOPSO algorithm is utilized for the purpose of achieving maximum power extraction from the output power produced by the WTS and PV by altering the duty cycle of the DC/DC converter connected to them. The battery controller ensures a consistent DC link of 400 V by using a bidirectional converter configuration. Based on the test findings, the MOPSO algorithm demonstrates superior power generation and performance than the P&O method. The MOPSO algorithm is able to effectively and efficiently extract maximum power from wind turbines or solar panels despite the presence of fluctuations in wind speed and irradiation levels. Subsequent research will focus on the development and

implementation of the MOPSO algorithm on a prototype hybrid system that utilizes embedded system technology.

ACKNOWLEDGMENTS

The authors would like to express their sincere gratitude to the Ministry of Education, Culture, Research, and Technology of Indonesia for the funding and support provided for this research. The authors also acknowledge the State Polytechnic of Malang for its valuable facilities, resources, and continuous encouragement throughout the completion of this work.

FUNDING INFORMATION

This work is supported by the Ministry of Education, Culture, Research, and Technology of Indonesia under the Fundamental Research scheme, with contract number 1022/PL2.1/HL/2022.

AUTHOR CONTRIBUTIONS STATEMENT

This journal uses the Contributor Roles Taxonomy (CRediT) to recognize individual author contributions, reduce authorship disputes, and facilitate collaboration.

Name of Author	C	M	So	Va	Fo	I	R	D	O	E	Vi	Su	P	Fu
Ratna Ika Putri	✓	✓	✓	✓	✓	✓		✓	✓	✓			✓	✓
Ferdian Ronilaya		✓				✓		✓	✓	✓	✓	✓		✓
Ika Noer Syamsiana			✓	✓		✓	✓			✓	✓		✓	✓
Zakiyah Amalia				✓	✓		✓	✓		✓	✓		✓	
Lie Jasa						✓				✓	✓	✓		

C : **C**onceptualization
M : **M**ethodology
So : **So**ftware
Va : **Va**lidation
Fo : **Fo**rmal analysis
I : **I**nvestigation
R : **R**esources
D : **D**ata Curation
O : Writing - **O**riginal Draft
E : Writing - Review & **E**diting
Vi : **Vi**sualization
Su : **Su**pervision
P : **P**roject administration
Fu : **Fu**nding acquisition

CONFLICT OF INTEREST STATEMENT

Authors state no conflict of interest.

DATA AVAILABILITY

Data availability is not relevant to this paper, as no new data were generated or analyzed during the course of this investigation.

REFERENCES

[1] M. M. R. Ahmed, "Mitigating uncertainty problems of renewable energy resources through efficient integration of hybrid solar PV/wind systems into power networks," *IEEE Access*, vol. 12, pp. 30311–30328, 2024, doi: 10.1109/ACCESS.2024.3370163z.
[2] M. Puianu, R. O. Flangea, N. Arghira, and S. S. Iliescu, "PV panel-wind turbine hybrid system modelling," *2017 21st International Conference on Control Systems and Computer Science (CSCS)*, 2017, pp. 636-640, doi: 10.1109/CSCS.2017.97.
[3] P. Roy, J. He, T. Zhao, and Y. V. Singh, "Recent advances of wind-solar hybrid renewable energy systems for power generation: a review," *IEEE Open Journal of the Industrial Electronics Society*, vol. 3, pp. 81–104, 2022, doi: 10.1109/OJIES.2022.3144093.
[4] H. Fathabadi, "Novel standalone hybrid solar/wind/fuel cell power generation system for remote areas," *Solar Energy*, vol. 146, pp. 30–43, 2017, doi: 10.1016/j.solener.2017.01.071.
[5] M. J. Khan and L. Mathew, "Comparative study of maximum power point tracking techniques for hybrid renewable energy system," *International Journal of Electronics*, vol. 106, no. 8, pp. 1216–1228, 2019, doi: 10.1080/00207217.2019.1584917.
[6] M. J. Khan, "Review of recent trends in optimization techniques for hybrid renewable energy system," *Archives of Computational Methods in Engineering*, vol. 28, no. 1, 2020, doi: 10.1007/s11831-020-09424-2.
[7] Y. Soufi, S. Kahla, and M. Bechouat, "Feedback linearization control based particle swarm optimization for maximum power point tracking of wind turbine equipped by PMSG connected to the grid," *International Journal Hydrogen Energy*, vol. 41, no. 45, pp. 20950–20955, 2016, doi: 10.1016/j.ijhydene.2016.06.010.
[8] L. G. Vasant and V. R. Pawar, "Solar-wind hybrid energi system using MPPT," *2017 International Conference on Intelligent Computing and Control Systems (ICICCS)*, pp. 595–597, 2017, doi: 10.1109/ICCONS.2017.8250531
[9] V. Khare, S. Nema, and P. Baredar, "Solar-wind hybrid renewable energy system: a review," *Renewable and Sustainable Energy Reviews*, vol. 58, pp. 23–33, 2016, doi: 10.1016/j.rser.2015.12.223.

[10] M. H. Ibrahim, S. P. Ang, M. N. Dani, M. I. Rahman, R. Petra, and S. M. Sulthan, "Optimizing step-size of perturb & observe and incremental conductance MPPT techniques using PSO for grid-tied PV system," *IEEE Access*, vol. 11, pp. 13079–13090, 2023, doi: 10.1109/ACCESS.2023.3242979.
[11] R. I. Putri, S. Wibowo, and M. Rifa'i, "Maximum power point tracking for photovoltaic using incremental conductance method," *Energy Procedia*, vol. 68, pp. 22–30, 2015, doi: 10.1016/j.egypro.2015.03.228.
[12] M. Rezkallah, A. Hamadi, A. Chandra, and B. Singh, "Design and implementation of active power control with improved p&o method for wind-PV-battery based standalone generation system," *IEEE Transactions on Industrial Electronics*, vol. 65, no. 7, pp. 5590–5600, 2018, doi: 10.1109/TIE.2017.2777404.
[13] R. I. Putri, M. Pujiantara, A. Priyadi, T. Ise, and M. H. Purnomo, "Maximum power extraction improvement using sensorless controller based on adaptive perturb and observe algorithm for PMSG wind turbine application," *IET Electric Power Applicatio*n, vol. 12, no. 4, pp. 455–462, 2018, doi: 10.1049/iet-epa.2017.0603.
[14] J. Ahmed and Z. Salam, "An enhanced adaptive P&O MPPT for fast and efficient tracking under varying environmental conditions," *IEEE Transactions on Sustainable Energy*, vol. 9, no. 3, pp. 1487–1496, 2018, doi: 10.1109/TSTE.2018.2791968.
[15] M. Alam *et al.*, "An adaptive power management approach for hybrid PV-wind desalination plant using recurrent neural networks," *Desalination*, vol. 569, p. 117038, 2024, doi: 10.1016/j.desal.2023.1170387.
[16] D. J. Petrović, M. M. Lazić, B. V. J. Lazić, B. D. Blanuša, and S. O. Aleksić, "Hybrid power supply system with fuzzy logic controller: power control algorithm, main properties, and applications," *Journal of Modern Power Systems and Clean Energy*, vol. 10, no. 4, pp. 923–931, Jul. 2022, doi: 10.35833/MPCE.2020.000069.
[17] R. I. Putri, M. Rifa'i, I. N. Syamsiana, and F. Ronilaya, "Control of PMSG stand-alone wind turbine system based on multi objective PSO," *International Journal of Renewable Energy Research*, vol. 10, no. 2, pp. 998–1004, 2020, doi:10.20508/ijrer.v10i2.10799.g7970.
[18] R. I. Putri, L. Jasa, M. Pujiantara, A. Priyadi, and M. H. Purnomo, "Tuning PI controller based on multiobjective optimization approaches for speed control of PMSG wind turbine," *International Review of Automatic Control*, vol. 8, no. 4, pp. 315–321, 2015, doi: 10.15866/ireaco.v8i4.7201.
[19] J. P. Ram, N. Rajasekar, and M. Miyatake, "Design and overview of maximum power point tracking techniques in wind and solar photovoltaic systems: a review," *Renewable and Sustainable Energy Reviews*, vol. 73, pp. 1138–1159, 2017, doi: 10.1016/j.rser.2017.02.009.
[20] M. Amer, A. Namaane, and N. K. M'sirdi, "Optimization of hybrid renewable energy systems (HRES) using PSO for cost reduction," *Energy Procedia*, vol. 42, pp. 318–327, 2013, doi: 10.1016/j.egypro.2013.11.032.
[21] A. F. Tazay, A. M. A. Ibrahim, O. Noureldeen, and I. Hamdan, "Modeling, control, and performance evaluation of grid-tied hybrid PV/wind power generation system: case study of Gabel El-Zeit Region, Egypt," *IEEE Access*, vol. 8, pp. 96528-96542, 2020, doi: 10.1109/ACCESS.2020.2993919
[22] M. M. Gulzar, A. Iqbal, D. Sibtain, and M. Khalid, "An innovative converterless solar PV control strategy for a grid connected hybrid PV/wind/fuel-cell system coupled with battery energy storage," *IEEE Access*, vol. 11, pp. 23245–23259, 2023, doi: 10.1109/ACCESS.2023.3252891.
[23] K. Anoune *et al.*, "Optimization and techno-economic analysis of photovoltaic-wind-battery based hybrid system," *Journal of Energy Storage*, vol. 32, p. 101878, 2020, doi: 10.1016/j.est.2020.101878.
[24] B. Tudu, K. K. Mandal, and N. Chakraborty, "Optimal design and development of PV-wind-battery based nano-grid system: A field-on-laboratory demonstration," *Frontiers in Energy*, vol. 13, pp. 269–283, 2019, doi: 10.1007/s11708-018-0573-z.
[25] A. A. Prasad, Y. Yang, M. Kay, C. Menictas, and S. Bremner, "Synergy of solar photovoltaics-wind-battery systems in Australia," *Renewable and Sustainable Energy Reviews*, vol. 152, p. 111693, 2021, doi: 10.1016/j.rser.2021.111693.

BIOGRAPHIES OF AUTHORS

Ratna Ika Putri was born in Balikpapan, East Borneo, Indonesia. She received Ph.D. degree from Institut Teknologi Sepuluh November (ITS), Indonesia in 2017. Her current research interest in control, power electronic, artificial intelligent, optimization for renewable energy system and renewable energy. She has been a Lecturer of Electrical Engineering, State Polytechnic of Malang since 2000. She can be contacted at email: ratna.ika@polinema.ac.id.

Ferdian Ronilaya was born in Malang, East Java, Indonesia. He received Ph.D. from Kumamoto University, Japan in 2015. His current research interests in control, power electronic, power quality, power driver, renewable energy, and power systems. He has been a Lecturer of Electrical Engineering, State Polytechnic of Malang since 2005. He can be contacted at email: ferdian@polinema.ac.id.

Ika Noer Syamsiana was born in Malang, East Java, Indonesia. She received Ph.D. from Southern Taiwan University of Science and Technology (STUST), Taiwan in 2017. Her current research interests in control, power electronic, artificial intelligence, power driver, renewable energy, and power systems. She has been a Lecturer of Electrical Engineering, State Polytechnic of Malang since 2002. She can be contacted at email: ikanoersyamsiana@polinema.ac.id.

Zakiyah Amalia was born in Malang, East Java, Indonesia. She received Master degree from Malang State Polytechnic, Indonesia in 2018. Her current research interest in control engineering. She has been a Lecturer of Electrical Engineering, State Polytechnic of Malang since 2019. She can be contacted at email: zakiyah_amalia@polinema.ac.id.

Lie Jasa was born in Tabanan, Indonesia. He received Ph.D. degree from Institut Teknologi Sepuluh November (ITS), Indonesia in 2015. His current research interests in renewable energy, micro-hydro, hydropower, computer network, and microprocessor applied. He has been a Lecturer of Electrical Engineering, Udayana University. He can be contacted at email: liejasa@unud.ac.id.